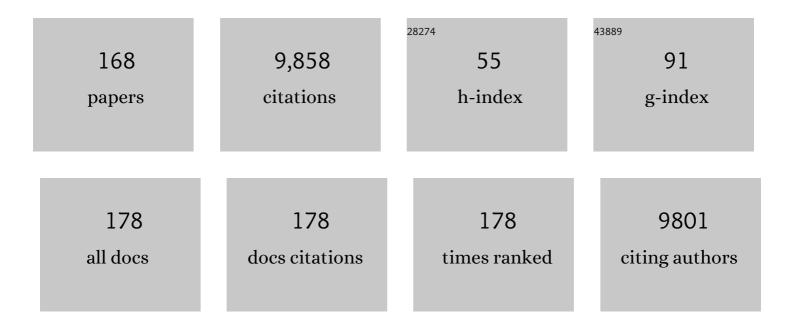
List of Publications by Year in descending order

Source: https://exaly.com/author-pdf/8067204/publications.pdf Version: 2024-02-01



FENC DINC

#	Article	IF	CITATIONS
1	Hydrophobic/Hydrophilic Ratio of Amphiphilic Helix Mimetics Determines the Effects on Islet Amyloid Polypeptide Aggregation. Journal of Chemical Information and Modeling, 2022, 62, 1760-1770.	5.4	9
2	Chemical and Biophysical Signatures of the Protein Corona in Nanomedicine. Journal of the American Chemical Society, 2022, 144, 9184-9205.	13.7	98
3	Substoichiometric Inhibition of Insulin against IAPP Aggregation Is Attenuated by the Incompletely Processed N-Terminus of proIAPP. ACS Chemical Neuroscience, 2022, 13, 2006-2016.	3.5	1
4	The Membrane Axis of Alzheimer's Nanomedicine. Advanced NanoBiomed Research, 2021, 1, 2000040.	3.6	12
5	Direct Observation of β-Barrel Intermediates in the Self-Assembly of Toxic SOD1 _{28–38} and Absence in Nontoxic Glycine Mutants. Journal of Chemical Information and Modeling, 2021, 61, 966-975.	5.4	14
6	Accelerated Amyloid Beta Pathogenesis by Bacterial Amyloid FapC. Biophysical Journal, 2021, 120, 31a.	0.5	0
7	Probing Interdomain Linkers and Protein Supertertiary Structure In Vitro and in Live Cells with Fluorescent Protein Resonance Energy Transfer. Journal of Molecular Biology, 2021, 433, 166793.	4.2	17
8	Ensemble switching unveils a kinetic rheostat mechanism of the eukaryotic thiamine pyrophosphate riboswitch. Rna, 2021, 27, 771-790.	3.5	15
9	Misfolding and Self-Assembly Dynamics of Microtubule-Binding Repeats of the Alzheimer-Related Protein Tau. Journal of Chemical Information and Modeling, 2021, 61, 2916-2925.	5.4	24
10	Spontaneous formation of β-sheet nano-barrels during the early aggregation of Alzheimer's amyloid beta. Nano Today, 2021, 38, 101125.	11.9	44
11	Ultrasmall Molybdenum Disulfide Quantum Dots Cage Alzheimer's Amyloid Beta to Restore Membrane Fluidity. ACS Applied Materials & Interfaces, 2021, 13, 29936-29948.	8.0	22
12	Inhibition of Amyloid Aggregation and Toxicity with Janus Iron Oxide Nanoparticles. Chemistry of Materials, 2021, 33, 6484-6500.	6.7	25
13	SAMase of Bacteriophage T3 Inactivates Escherichia coli's Methionine <i>S</i> -Adenosyltransferase by Forming Heteropolymers. MBio, 2021, 12, e0124221.	4.1	5
14	Out-of-Equilibrium Biophysical Chemistry: The Case for Multidimensional, Integrated Single-Molecule Approaches. Journal of Physical Chemistry B, 2021, 125, 10404-10418.	2.6	9
15	A Framework of Paracellular Transport via Nanoparticlesâ€Induced Endothelial Leakiness. Advanced Science, 2021, 8, e2102519.	11.2	22
16	Amyloid Aggregation under the Lens of Liquid–Liquid Phase Separation. Journal of Physical Chemistry Letters, 2021, 12, 368-378.	4.6	34
17	Integrative structural dynamics probing of the conformational heterogeneity in synaptosomal-associated protein 25. Cell Reports Physical Science, 2021, 2, 100616.	5.6	9
18	A buried glutamate in the cross-β core renders β-endorphin fibrils reversible. Nanoscale, 2021, 13, 19593-19603.	5.6	4

#	Article	IF	CITATIONS
19	Graphene quantum dots obstruct the membrane axis of Alzheimer's amyloid beta. Physical Chemistry Chemical Physics, 2021, 24, 86-97.	2.8	14
20	Dynamic Protein Corona of Gold Nanoparticles with an Evolving Morphology. ACS Applied Materials & Interfaces, 2021, 13, 58238-58251.	8.0	23
21	Mitigation of Amyloidosis with Nanomaterials. Advanced Materials, 2020, 32, e1901690.	21.0	87
22	Human Plasma Protein Corona of Aβ Amyloid and Its Impact on Islet Amyloid Polypeptide Cross-Seeding. Biomacromolecules, 2020, 21, 988-998.	5.4	15
23	Amyloid Beta Pathogenesis: Accelerated Amyloid Beta Pathogenesis by Bacterial Amyloid FapC (Adv. Sci.) Tj ETQ	q1 1 0.78 11.2	4314 rgBT /
24	Accelerated Amyloid Beta Pathogenesis by Bacterial Amyloid FapC. Advanced Science, 2020, 7, 2001299.	11.2	47
25	Amyloidosis inhibition, a new frontier of the protein corona. Nano Today, 2020, 35, 100937.	11.9	32
26	Interdomain Dynamics Underlie Function and Regulation of Postsynaptic Density Protein 95. Biophysical Journal, 2020, 118, 336a.	0.5	0
27	Dynamic Organization in the Supertertiary Structure of PDZ3-SH3-GuK Core Supramodule of PSD-95 Scaffold Protein. Biophysical Journal, 2020, 118, 206a.	0.5	0
28	αB-Crystallin Chaperone Inhibits Aβ Aggregation by Capping the β-Sheet-Rich Oligomers and Fibrils. Journal of Physical Chemistry B, 2020, 124, 10138-10146.	2.6	13
29	Amyloidosis: Mitigation of Amyloidosis with Nanomaterials (Adv. Mater. 18/2020). Advanced Materials, 2020, 32, 2070146.	21.0	2
30	Elevated amyloidoses of human IAPP and amyloid beta by lipopolysaccharide and their mitigation by carbon quantum dots. Nanoscale, 2020, 12, 12317-12328.	5.6	23
31	Morphological Determinants of Carbon Nanomaterial-Induced Amyloid Peptide Self-Assembly. Frontiers in Chemistry, 2020, 8, 160.	3.6	4
32	RNA-Puzzles Round IV: 3D structure predictions of four ribozymes and two aptamers. Rna, 2020, 26, 982-995.	3.5	100
33	Quantitative Fluorescence Quenching by Aromatic Amino Acids. Biophysical Journal, 2020, 118, 472a.	0.5	0
34	Thermo- and pH-responsive fibrillization of squid suckerin A1H1 peptide. Nanoscale, 2020, 12, 6307-6317.	5.6	19
35	Nanosilver Mitigates Biofilm Formation via FapC Amyloidosis Inhibition. Small, 2020, 16, e1906674.	10.0	26
36	Single-Molecular Heteroamyloidosis of Human Islet Amyloid Polypeptide. Nano Letters, 2019, 19, 6535-6546.	9.1	27

#	Article	IF	CITATIONS
37	Inhibition of amyloid beta toxicity in zebrafish with a chaperone-gold nanoparticle dual strategy. Nature Communications, 2019, 10, 3780.	12.8	132
38	Graphene quantum dots rescue protein dysregulation of pancreatic β-cells exposed to human islet amyloid polypeptide. Nano Research, 2019, 12, 2827-2834.	10.4	34
39	Amphiphilic surface chemistry of fullerenols is necessary for inhibiting the amyloid aggregation of alpha-synuclein NACore. Nanoscale, 2019, 11, 11933-11945.	5.6	47
40	Peptide Selfâ€Assembly: Amyloid Selfâ€Assembly of hIAPP8â€20 via the Accumulation of Helical Oligomers, αâ€Helix to βâ€Sheet Transition, and Formation of βâ€Barrel Intermediates (Small 18/2019). Small, 2019, 15, 1970093.	10.0	1
41	Amyloid Selfâ€Assembly of hIAPP8â€20 via the Accumulation of Helical Oligomers, αâ€Helix to βâ€Sheet Transition, and Formation of βâ€Barrel Intermediates. Small, 2019, 15, e1805166.	10.0	49
42	Physical and toxicological profiles of human IAPP amyloids and plaques. Science Bulletin, 2019, 64, 26-35.	9.0	24
43	Nucleation of β-rich oligomers and β-barrels in the early aggregation of human islet amyloid polypeptide. Biochimica Et Biophysica Acta - Molecular Basis of Disease, 2019, 1865, 434-444.	3.8	44
44	The capricious electrostatic force: Revealing the signaling pathway in integrin α2-l domain. Journal of Theoretical and Computational Chemistry, 2018, 17, 1840001.	1.8	3
45	Islet Amyloid Polypeptide Promotes Amyloid-Beta Aggregation by Binding-Induced Helix-Unfolding of the Amyloidogenic Core. ACS Chemical Neuroscience, 2018, 9, 967-975.	3.5	39
46	Oligomerization and Fibrillization Dynamics of Amyloid Peptides and BETA-Barrel Oligomer Intermediates. Biophysical Journal, 2018, 114, 227a-228a.	0.5	0
47	Structures and dynamics of β-barrel oligomer intermediates of amyloid-beta16-22 aggregation. Biochimica Et Biophysica Acta - Biomembranes, 2018, 1860, 1687-1697.	2.6	27
48	Nanoscale inhibition of polymorphic and ambidextrous IAPP amyloid aggregation with small molecules. Nano Research, 2018, 11, 3636-3647.	10.4	35
49	Graphene quantum dots against human IAPP aggregation and toxicity <i>in vivo</i> . Nanoscale, 2018, 10, 19995-20006.	5.6	100
50	Transient Interactions in Multidomain Proteins Identified by FRET. Biophysical Journal, 2018, 114, 565a.	0.5	0
51	Mitigating Human IAPP Amyloidogenesis In Vivo with Chiral Silica Nanoribbons. Small, 2018, 14, e1802825.	10.0	57
52	Identifying weak interdomain interactions that stabilize the supertertiary structure of the N-terminal tandem PDZ domains of PSD-95. Nature Communications, 2018, 9, 3724.	12.8	41
53	Profiling the Serum Protein Corona of Fibrillar Human Islet Amyloid Polypeptide. ACS Nano, 2018, 12, 6066-6078.	14.6	39
54	Understanding Effects of PAMAM Dendrimer Size and Surface Chemistry on Serum Protein Binding with Discrete Molecular Dynamics Simulations. ACS Sustainable Chemistry and Engineering, 2018, 6, 11704-11715.	6.7	41

#	Article	IF	CITATIONS
55	β-barrel Oligomers as Common Intermediates of Peptides Self-Assembling into Cross-β Aggregates. Scientific Reports, 2018, 8, 10353.	3.3	62
56	Nonnative Energetic Frustrations in Protein Folding at Residual Level: A Simulation Study of Homologous Immunoglobulin-like β-Sandwich Proteins. International Journal of Molecular Sciences, 2018, 19, 1515.	4.1	1
57	Effect of Bio-molecules on Human Islet Amyloid Polypeptide Aggregation, Fibril Remodeling and Cytoxicity. Biophysical Journal, 2018, 114, 228a.	0.5	0
58	RNA-Puzzles Round III: 3D RNA structure prediction of five riboswitches and one ribozyme. Rna, 2017, 23, 655-672.	3.5	158
59	Brushed Polyethylene Glycol and Phosphorylcholine as Promising Grafting Agents against Protein Binding. Biophysical Journal, 2017, 112, 350a.	0.5	0
60	NanoEHS beyond toxicity – focusing on biocorona. Environmental Science: Nano, 2017, 4, 1433-1454.	4.3	43
61	Mesoscopic Properties and Molecular Mechanisms of IAPP Amyloid Inhibition and Remodeling with Small Molecules. Biophysical Journal, 2017, 112, 340a.	0.5	0
62	Dynamic Equilibrium of the TPP Riboswitch as Observed by MFD Fret. Biophysical Journal, 2017, 112, 368a.	0.5	0
63	Distinct oligomerization and fibrillization dynamics of amyloid core sequences of amyloid-beta and islet amyloid polypeptide. Physical Chemistry Chemical Physics, 2017, 19, 28414-28423.	2.8	43
64	Star Polymers Reduce Islet Amyloid Polypeptide Toxicity via Accelerated Amyloid Aggregation. Biomacromolecules, 2017, 18, 4249-4260.	5.4	65
65	Probing the modulated formation of gold nanoparticles–beta-lactoglobulin corona complexes and their applications. Nanoscale, 2017, 9, 17758-17769.	5.6	21
66	Zinc-coordination and C-peptide complexation: a potential mechanism for the endogenous inhibition of IAPP aggregation. Chemical Communications, 2017, 53, 9394-9397.	4.1	21
67	Modulating protein amyloid aggregation with nanomaterials. Environmental Science: Nano, 2017, 4, 1772-1783.	4.3	38
68	Lysophosphatidylcholine modulates the aggregation of human islet amyloid polypeptide. Physical Chemistry Chemical Physics, 2017, 19, 30627-30635.	2.8	12
69	Cofibrillization of Pathogenic and Functional Amyloid Proteins with Gold Nanoparticles against Amyloidogenesis. Biomacromolecules, 2017, 18, 4316-4322.	5.4	50
70	Implications of peptide assemblies in amyloid diseases. Chemical Society Reviews, 2017, 46, 6492-6531.	38.1	262
71	Mechanistic Insights from Discrete Molecular Dynamics Simulations of Pesticide–Nanoparticle Interactions. Environmental Science & Technology, 2017, 51, 8396-8404.	10.0	22
72	Effects of Protein Corona on IAPP Amyloid Aggregation, Fibril Remodelling, and Cytotoxicity. Scientific Reports, 2017, 7, 2455.	3.3	34

#	Article	IF	CITATIONS
73	Structure modeling of RNA using sparse NMR constraints. Nucleic Acids Research, 2017, 45, 12638-12647.	14.5	15
74	Stabilizing Off-pathway Oligomers by Polyphenol Nanoassemblies for IAPP Aggregation Inhibition. Scientific Reports, 2016, 6, 19463.	3.3	104
75	Multiscale Modeling of Dendrimers for Biological Applications. Biophysical Journal, 2016, 110, 546a.	0.5	0
76	Brushed polyethylene glycol and phosphorylcholine for grafting nanoparticles against protein binding. Polymer Chemistry, 2016, 7, 6875-6879.	3.9	20
77	A hidden aggregationâ€prone structure in the heart of hypoxia inducible factor prolyl hydroxylase. Proteins: Structure, Function and Bioinformatics, 2016, 84, 611-623.	2.6	2
78	Inhibition of hIAPP Amyloid Aggregation and Pancreatic β-Cell Toxicity by OH-Terminated PAMAM Dendrimer. Small, 2016, 12, 1615-1626.	10.0	99
79	Graphene oxide inhibits hIAPP amyloid fibrillation and toxicity in insulin-producing NIT-1 cells. Physical Chemistry Chemical Physics, 2016, 18, 94-100.	2.8	70
80	Synthesis and in vitro properties of iron oxide nanoparticles grafted with brushed phosphorylcholine and polyethylene glycol. Polymer Chemistry, 2016, 7, 1931-1944.	3.9	32
81	CSAR Benchmark of Flexible MedusaDock in Affinity Prediction and Nativelike Binding Pose Selection. Journal of Chemical Information and Modeling, 2016, 56, 1042-1052.	5.4	20
82	Striped Nanoparticles: A Thermodynamics Model for the Emergence of a Stripeâ€like Binary SAM on a Nanoparticle Surface (Small 37/2015). Small, 2015, 11, 4798-4798.	10.0	0
83	A Thermodynamics Model for the Emergence of a Stripeâ€like Binary SAM on a Nanoparticle Surface. Small, 2015, 11, 4894-4899.	10.0	21
84	Promotion or Inhibition of Islet Amyloid Polypeptide Aggregation by Zinc Coordination Depends on Its Relative Concentration. Biochemistry, 2015, 54, 7335-7344.	2.5	27
85	Inhibition of IAPP aggregation by insulin depends on the insulin oligomeric state regulated by zinc ion concentration. Scientific Reports, 2015, 5, 8240.	3.3	50
86	Deviation from the Unimolecular Micelle Paradigm of PAMAM Dendrimers Induced by Strong Interligand Interactions. Journal of Physical Chemistry C, 2015, 119, 19475-19484.	3.1	6
87	PAMAM Dendrimers and Graphene: Materials for Removing Aromatic Contaminants from Water. Environmental Science & Technology, 2015, 49, 4490-4497.	10.0	40
88	<i>RNA-Puzzles</i> Round II: assessment of RNA structure prediction programs applied to three large RNA structures. Rna, 2015, 21, 1066-1084.	3.5	161
89	Contrasting effects of nanoparticle–protein attraction on amyloid aggregation. RSC Advances, 2015, 5, 105489-105498.	3.6	56
90	Thermostability and reversibility of silver nanoparticle–protein binding. Physical Chemistry Chemical Physics, 2015, 17, 1728-1739.	2.8	30

#	Article	IF	CITATIONS
91	PostÂtranslational Modifications Promote Formation of SOD1 Oligomers With Potential Toxicity in ALS. FASEB Journal, 2015, 29, 564.1.	0.5	0
92	Structural and energetic determinants of tyrosylprotein sulfotransferase sulfation specificity. Bioinformatics, 2014, 30, 2302-2309.	4.1	7
93	Computational approaches to understanding protein aggregation in neurodegeneration. Journal of Molecular Cell Biology, 2014, 6, 104-115.	3.3	43
94	Structure–Function Relationship of PAMAM Dendrimers as Robust Oil Dispersants. Environmental Science & Technology, 2014, 48, 12868-12875.	10.0	21
95	RNA Tertiary Structure Analysis by 2′-Hydroxyl Molecular Interference. Biochemistry, 2014, 53, 6825-6833.	2.5	17
96	Effect of fullerenol surface chemistry on nanoparticle binding-induced protein misfolding. Nanoscale, 2014, 6, 8340-8349.	5.6	41
97	Labeling native bacterial RNA in live cells. Cell Research, 2014, 24, 894-897.	12.0	15
98	Predicting Binding Affinity of CSAR Ligands Using Both Structure-Based and Ligand-Based Approaches. Journal of Chemical Information and Modeling, 2013, 53, 1915-1922.	5.4	20
99	Direct observation of a single nanoparticle–ubiquitin corona formation. Nanoscale, 2013, 5, 9162.	5.6	116
100	Competitive Binding of Natural Amphiphiles with Graphene Derivatives. Scientific Reports, 2013, 3, 2273.	3.3	61
101	Interaction of firefly luciferase and silver nanoparticles and its impact on enzyme activity. Nanotechnology, 2013, 24, 345101.	2.6	47
102	Rational Design of a Ligand-Controlled Protein Conformational Switch. Biophysical Journal, 2013, 104, 18a-19a.	0.5	0
103	Incorporating Backbone Flexibility in MedusaDock Improves Ligand-Binding Pose Prediction in the CSAR2011 Docking Benchmark. Journal of Chemical Information and Modeling, 2013, 53, 1871-1879.	5.4	37
104	Statistical Analysis of SHAPE-Directed RNA Secondary Structure Modeling. Biochemistry, 2013, 52, 596-599.	2.5	14
105	Submillisecond Elastic Recoil Reveals Molecular Origins of Fibrin Fiber Mechanics. Biophysical Journal, 2013, 104, 2671-2680.	0.5	35
106	Rational design of a ligand-controlled protein conformational switch. Proceedings of the National Academy of Sciences of the United States of America, 2013, 110, 6800-6804.	7.1	111
107	Binding of cytoskeletal proteins with silver nanoparticles. RSC Advances, 2013, 3, 22002.	3.6	36
108	<i>RNA-Puzzles</i> : A CASP-like evaluation of RNA three-dimensional structure prediction. Rna, 2012, 18, 610-625.	3.5	241

#	Article	IF	CITATIONS
109	Harnessing a Physiologic Mechanism for siRNA Delivery With Mimetic Lipoprotein Particles. Molecular Therapy, 2012, 20, 1582-1589.	8.2	65
110	New Models of Tetrahymena Telomerase RNA from Experimentally Derived Constraints and Modeling. Journal of the American Chemical Society, 2012, 134, 20070-20080.	13.7	19
111	Discrete Molecular Dynamics Simulation of Biomolecules. Biological and Medical Physics Series, 2012, , 55-73.	0.4	13
112	Local Unfolding of Cu, Zn Superoxide Dismutase Monomer Determines the Morphology of Fibrillar Aggregates. Journal of Molecular Biology, 2012, 421, 548-560.	4.2	74
113	Hybrid Dynamics Simulation Engine for Metalloproteins. Biophysical Journal, 2012, 103, 767-776.	0.5	26
114	Discrete Molecular Dynamics: An Efficient And Versatile Simulation Method For Fine Protein Characterization. Journal of Physical Chemistry B, 2012, 116, 8375-8382.	2.6	179
115	Multiscale Modeling of RNA Structure and Dynamics. Nucleic Acids and Molecular Biology, 2012, , 167-184.	0.2	3
116	Three-dimensional RNA structure refinement by hydroxyl radical probing. Nature Methods, 2012, 9, 603-608.	19.0	77
117	Structural and Thermodynamic Effects of Post-translational Modifications in Mutant and Wild Type Cu, Zn Superoxide Dismutase. Journal of Molecular Biology, 2011, 408, 555-567.	4.2	43
118	Structural Basis for μ-Opioid Receptor Binding and Activation. Structure, 2011, 19, 1683-1690.	3.3	30
119	Structural and Dynamic Determinants of Protein-Peptide Recognition. Structure, 2011, 19, 1837-1845.	3.3	79
120	Discrete molecular dynamics. Wiley Interdisciplinary Reviews: Computational Molecular Science, 2011, 1, 80-92.	14.6	91
121	Automated minimization of steric clashes in protein structures. Proteins: Structure, Function and Bioinformatics, 2011, 79, 261-270.	2.6	372
122	Gaia: automated quality assessment of protein structure models. Bioinformatics, 2011, 27, 2209-2215.	4.1	44
123	Nâ€ŧerminal strands of filamin Ig domains act as a conformational switch under biological forces. Proteins: Structure, Function and Bioinformatics, 2010, 78, 12-24.	2.6	29
124	Engineered allosteric activation of kinases in living cells. Nature Biotechnology, 2010, 28, 743-747.	17.5	177
125	Robust and Generic RNA Modeling Using Inferred Constraints: A Structure for the Hepatitis C Virus IRES Pseudoknot Domain. Biochemistry, 2010, 49, 4931-4933.	2.5	31
126	On the significance of an RNA tertiary structure prediction. Rna, 2010, 16, 1340-1349.	3.5	103

#	Article	IF	CITATIONS
127	Rapid Flexible Docking Using a Stochastic Rotamer Library of Ligands. Journal of Chemical Information and Modeling, 2010, 50, 1623-1632.	5.4	80
128	Computational Evaluation of Protein Stability Change upon Mutations. Methods in Molecular Biology, 2010, 634, 189-201.	0.9	7
129	Polyglutamine Induced Misfolding of Huntingtin Exon1 is Modulated by the Flanking Sequences. PLoS Computational Biology, 2010, 6, e1000772.	3.2	86
130	G Protein Mono-ubiquitination by the Rsp5 Ubiquitin Ligase. Journal of Biological Chemistry, 2009, 284, 8940-8950.	3.4	25
131	Community-wide assessment of GPCR structure modelling and ligand docking: GPCR Dock 2008. Nature Reviews Drug Discovery, 2009, 8, 455-463.	46.4	260
132	Native-like RNA Tertiary Structures Using a Sequence-Encoded Cleavage Agent and Refinement by Discrete Molecular Dynamics. Journal of the American Chemical Society, 2009, 131, 2541-2546.	13.7	65
133	Ab Initio Folding of Proteins with All-Atom Discrete Molecular Dynamics. Structure, 2008, 16, 1010-1018.	3.3	287
134	Protein folding: Then and now. Archives of Biochemistry and Biophysics, 2008, 469, 4-19.	3.0	88
135	Dynamical roles of metal ions and the disulfide bond in Cu, Zn superoxide dismutase folding and aggregation. Proceedings of the National Academy of Sciences of the United States of America, 2008, 105, 19696-19701.	7.1	131
136	Ab initio RNA folding by discrete molecular dynamics: From structure prediction to folding mechanisms. Rna, 2008, 14, 1164-1173.	3.5	258
137	iFoldRNA: three-dimensional RNA structure prediction and folding. Bioinformatics, 2008, 24, 1951-1952.	4.1	200
138	Active Nuclear Receptors Exhibit Highly Correlated AF-2 Domain Motions. PLoS Computational Biology, 2008, 4, e1000111.	3.2	42
139	Probing protein aggregation using discrete molecular dynamics. Frontiers in Bioscience - Landmark, 2008, Volume, 4795.	3.0	21
140	The Length Dependence of the PolyQ-mediated Protein Aggregation. Journal of Biological Chemistry, 2007, 282, 25487-25492.	3.4	40
141	Parallel Folding Pathways in the SH3 Domain Protein. Journal of Molecular Biology, 2007, 373, 1348-1360.	4.2	29
142	Fidelity of the Protein Structure Reconstruction from Inter-Residue Proximity Constraints. Journal of Physical Chemistry B, 2007, 111, 7432-7438.	2.6	23
143	Multiscale Modeling of Nucleosome Dynamics. Biophysical Journal, 2007, 92, 1457-1470.	0.5	104
144	Eris: an automated estimator of protein stability. Nature Methods, 2007, 4, 466-467.	19.0	355

#	Article	IF	CITATIONS
145	Modeling Backbone Flexibility Improves Protein Stability Estimation. Structure, 2007, 15, 1567-1576.	3.3	147
146	Topological Determinants of Protein Domain Swapping. Structure, 2006, 14, 5-14.	3.3	73
147	Emergence of Protein Fold Families through Rational Design. PLoS Computational Biology, 2006, 2, e85.	3.2	177
148	iFold: a platform for interactive folding simulations of proteins. Bioinformatics, 2006, 22, 2693-2694.	4.1	27
149	A structural model reveals energy transduction in dynein. Proceedings of the National Academy of Sciences of the United States of America, 2006, 103, 18540-18545.	7.1	34
150	Fast complementation of split fluorescent protein triggered by DNA hybridization. Proceedings of the National Academy of Sciences of the United States of America, 2006, 103, 2052-2056.	7.1	73
151	Scaling Behavior and Structure of Denatured Proteins. Structure, 2005, 13, 1047-1054.	3.3	58
152	Simple but predictive protein models. Trends in Biotechnology, 2005, 23, 450-455.	9.3	73
153	Molecular Origin of Polyglutamine Aggregation in Neurodegenerative Diseases. PLoS Computational Biology, 2005, 1, e30.	3.2	92
154	Direct Observation of Protein Folding, Aggregation, and a Prion-like Conformational Conversion. Journal of Biological Chemistry, 2005, 280, 40235-40240.	3.4	77
155	Reconstruction of the src-SH3 Protein Domain Transition State Ensemble using Multiscale Molecular Dynamics Simulations. Journal of Molecular Biology, 2005, 350, 1035-1050.	4.2	72
156	Folding Trp-Cage to NMR Resolution Native Structure Using a Coarse-Grained Protein Model. Biophysical Journal, 2005, 88, 147-155.	0.5	130
157	Discrete molecular dynamics simulations of peptide aggregation. Physical Review E, 2004, 69, 041908.	2.1	74
158	New Insights into FAK Signaling and Localization Based on Detection of a FAT Domain Folding Intermediate. Structure, 2004, 12, 2161-2171.	3.3	62
159	Multiple Folding Pathways of the SH3 Domain. Biophysical Journal, 2004, 87, 521-533.	0.5	38
160	Molecular Dynamics Simulation of Amyloid \hat{l}^2 Dimer Formation. Biophysical Journal, 2004, 87, 2310-2321.	0.5	194
161	Mechanism for the ?-helix to ?-hairpin transition. Proteins: Structure, Function and Bioinformatics, 2003, 53, 220-228.	2.6	252
162	Folding of Cu, Zn Superoxide Dismutase and Familial Amyotrophic Lateral Sclerosis. Journal of Molecular Biology, 2003, 334, 515-525.	4.2	59

#	Article	IF	CITATIONS
163	Identifying Importance of Amino Acids for Protein Folding from Crystal Structures. Methods in Enzymology, 2003, 374, 616-638.	1.0	12
164	Topological determinants of protein folding. Proceedings of the National Academy of Sciences of the United States of America, 2002, 99, 8637-8641.	7.1	278
165	Molecular Dynamics Simulation of the SH3 Domain Aggregation Suggests a Generic Amyloidogenesis Mechanism. Journal of Molecular Biology, 2002, 324, 851-857.	4.2	157
166	Direct Molecular Dynamics Observation of Protein Folding Transition State Ensemble. Biophysical Journal, 2002, 83, 3525-3532.	0.5	133
167	Novel application of a perturbed photonic crystal: High-quality filter. Applied Physics Letters, 1997, 71, 2889-2891.	3.3	46
168	Integrative Structural Dynamics Probing of the Conformational Heterogeneity in Synaptosomal-Associated Protein 25. SSRN Electronic Journal, 0, , .	0.4	0